Supplemental Information

Palmitoylation couples insulin hypersecretion with β-cell failure in diabetes

Guifang Dong,[1,2] Sangeeta Adak,[1] George Spyropoulos,[3] Qiang Zhang,[1] Chu Feng,[1] Li Yin,[1] Sarah L. Speck,[1] Zeenat Shyr,[1] Shuntaro Morikawa,[1] Rie Asada Kitamura,[1] Rahul S. Kathayat,[4] Bryan C. Dickinson,[4] Xue Wen Ng,[5] David W. Piston,[5] Fumihiko Urano,[1,6] Maria S. Remedi,[1,5] Xiaochao Wei,[1] Clay F. Semenkovich[1,5,7]

[1]Division of Endocrinology, Metabolism & Lipid Research, Washington University, St. Louis, MO 63110
[2]Hubei Key Laboratory of Animal Nutrition and Feed Science, Wuhan Polytechnic University, Wuhan 430023, China
[3]Department of Pediatrics, Washington University, St. Louis, MO 63110
[4]Department of Chemistry, University of Chicago, Chicago, IL 60637
[5]Department of Cell Biology & Physiology, Washington University, St. Louis, MO 63110
[6]Department of Pathology & Immunology, Washington University, St. Louis, MO 63110
[7]Lead Contact

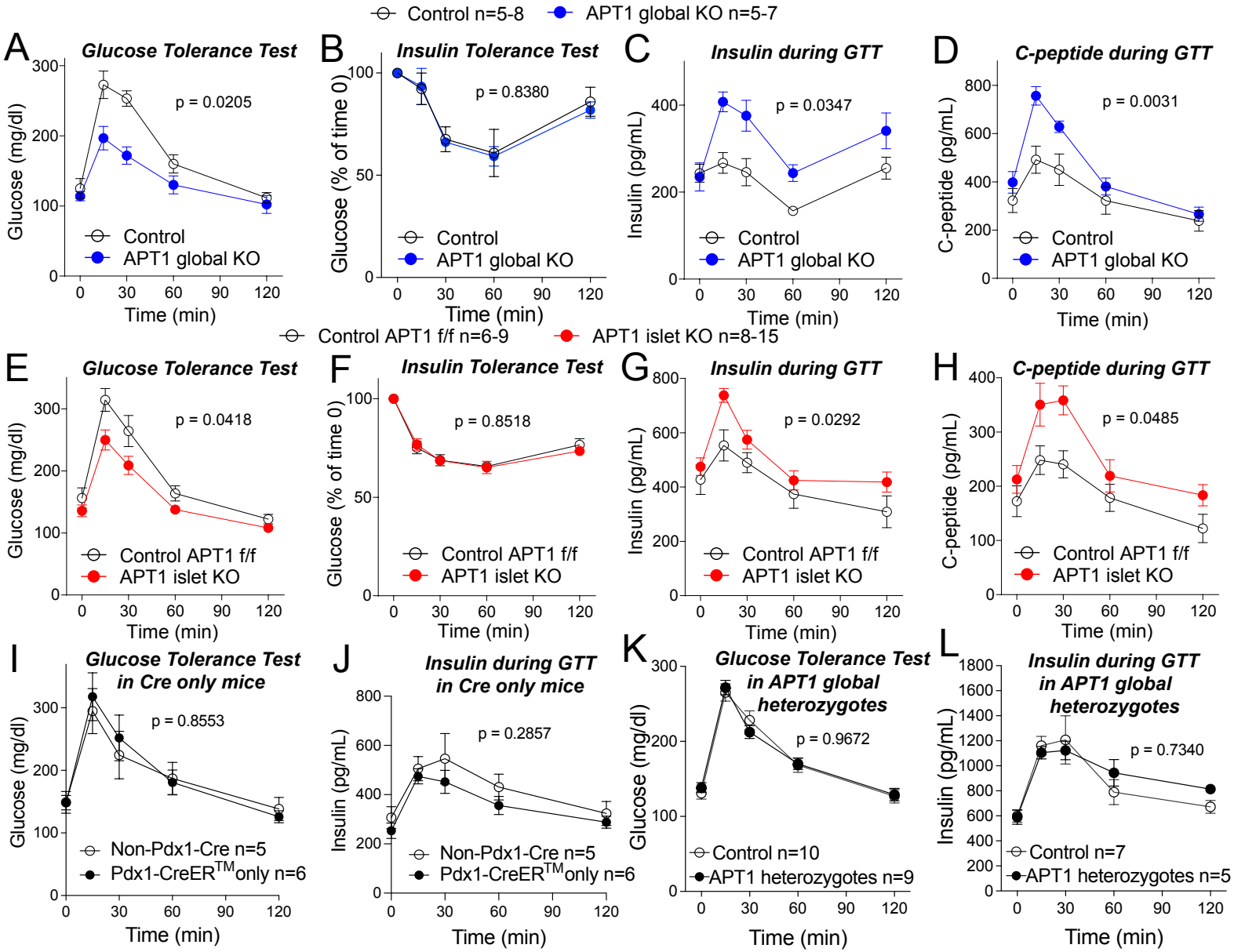

Figure S1. Related to Figure 2. APT1 deficiency in mice is associated with enhanced glucose tolerance due to increased insulin secretion. (A-D) Male and female APT1 global KO vs littermate control mice glucose tolerance tests, insulin tolerance tests, and insulin as well as C-peptide levels during glucose tolerance testing. (E-H) Male APT1 islet KO vs. littermate control floxed mice (without Cre) glucose tolerance tests, insulin tolerance tests, and insulin as well as C-peptide levels during glucose tolerance testing. (I,J) Glucose tolerance and insulin levels during glucose tolerance testing in male mice bearing the inducible Cre without the floxed alleles as compared to mice without Cre and without floxed alleles after being treated with tamoxifen. (K,L) Glucose tolerance and insulin levels during glucose tolerance testing in APT1 global heterozygotes.

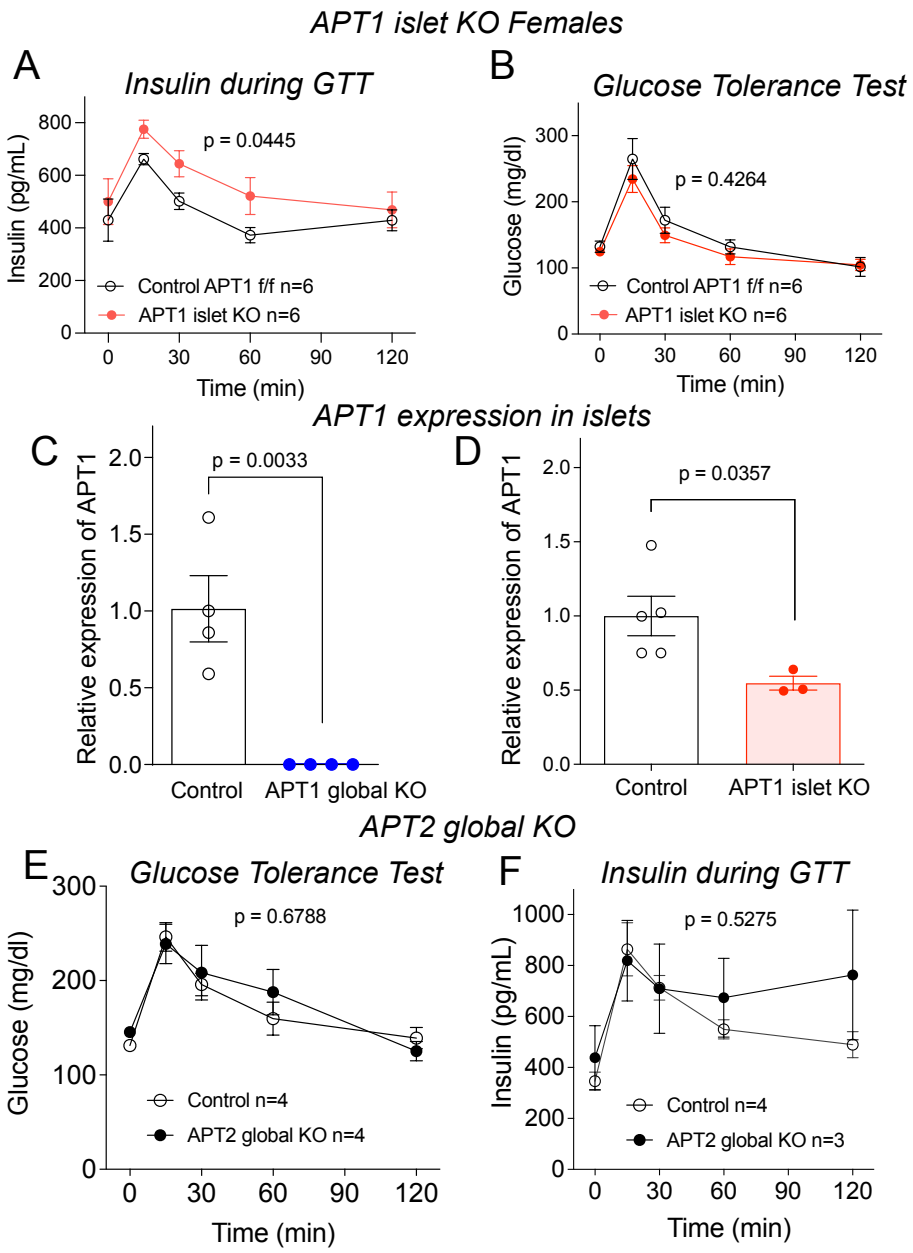

Figure S2. Related to Figure 2. Metabolic characterization of female APT1 islet KO mice, APT1 expression in islets, and metabolic characterization of APT2 global KO mice. (A) Insulin levels during glucose tolerance testing and (B) glucose tolerance testing in female APT1 islet KO mice. (C) APT1 mRNA assayed by semiquantitative RT-PCR in isolated islets from APT1 global knockout mice and littermate controls. (D) APT1 mRNA assayed by semiquantitative RT-PCR in isolated islets from APT1 islet knockout mice and littermate controls. (E) Glucose tolerance testing and (F) insulin levels during glucose tolerance testing in APT2 global KO mice.

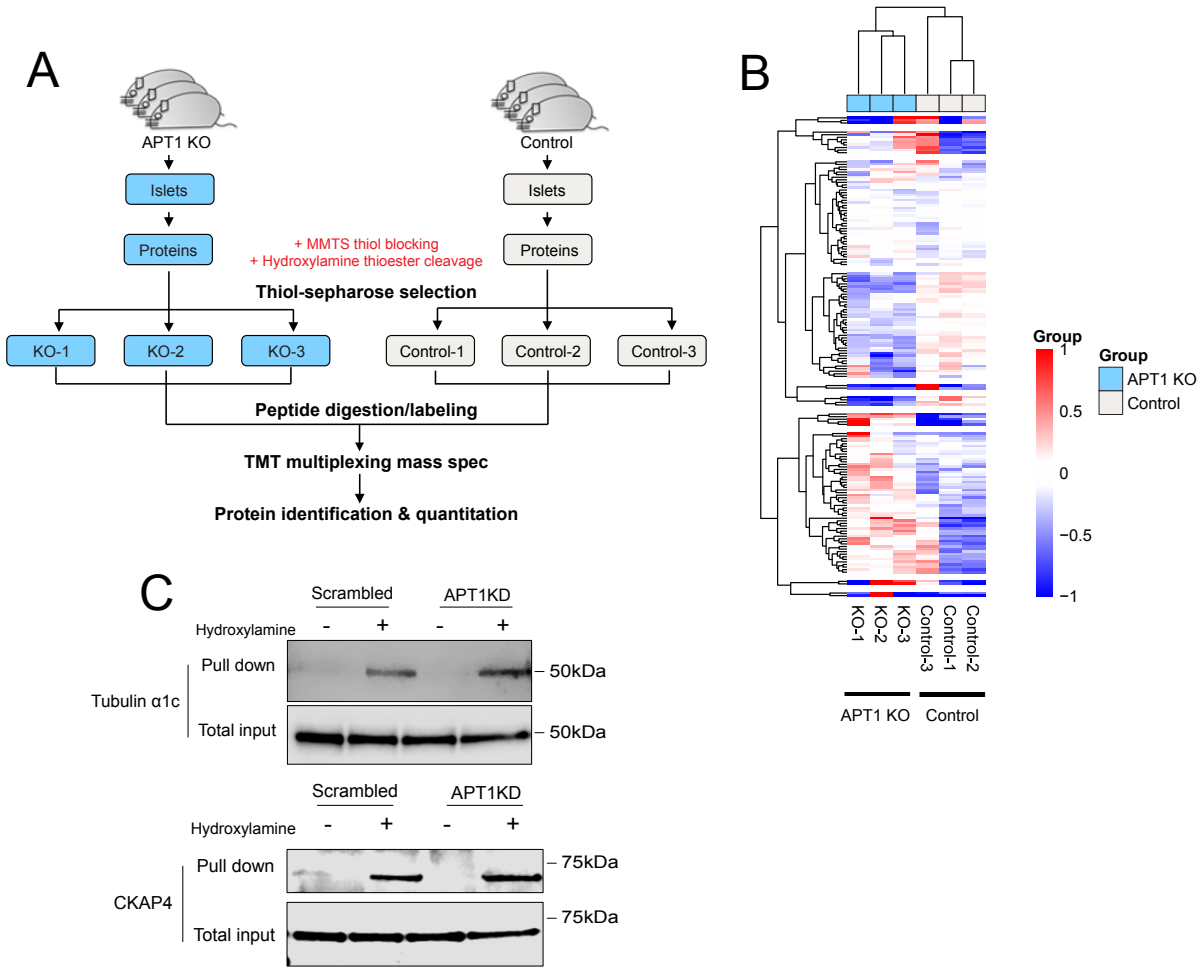

Figure S3. Related to Figure 4. Proteomic identification of candidate APT1 substrates in pancreatic islets. (A) Screening strategy for palmitoylated proteins increased in abundance in APT1 knockout as compared to control islets. (B) Heat map plot depicting relative protein palmitoylation levels between control and APT1 knockout islets. Vertical and horizontal dendrograms correspond to the protein and sample hierarchical clustering, respectively. (C) Validation of tubulin α1c (top) and CKAP4 (bottom) as S-palmitoylated proteins by resin-assisted capture (RAC) assay in control (Scrambled) and APT1 knockdown INS-1 cells.

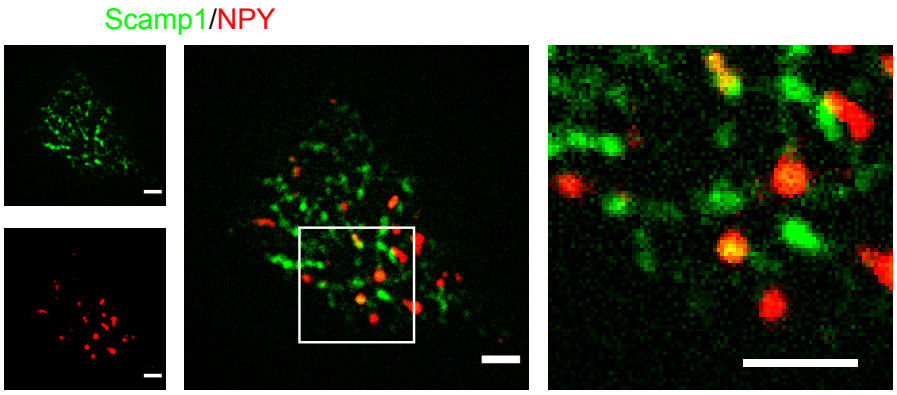

Figure S4. Related to Figure 4. Scamp1 partially localizes to secretory granules in INS-1 cells. Imaging of GFP-Scamp1 (green) and mCherry-NPY (red) granules in INS-1 cells by TIRF. The box in the merged image of the middle panel is shown at higher magnification in the right panel. Scale=2 μm.

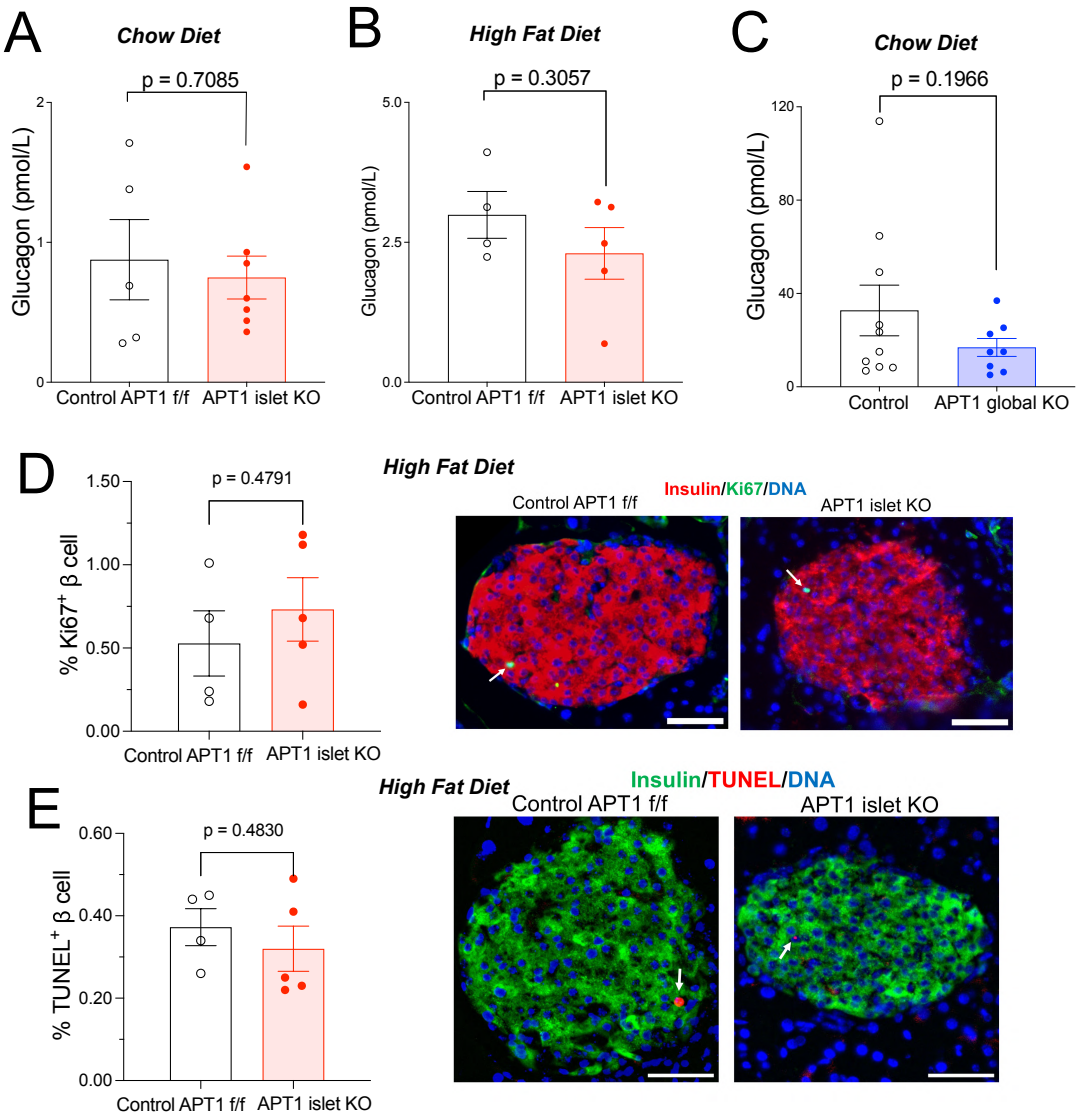

Figure S5. Related to Figure 5. Glucagon levels in mouse models, and proliferation as well as apoptosis in islets. (A-C) Plasma glucagon in controls and APT1 islet KO male mice on chow diet (A), controls and APT1 islet KO male mice on high fat diet (B), and controls and APT1 global KO mice of both sexes on chow diet (C). (D) Analysis of high fat fed control and APT1 islet KO mice for percentage of Ki67 positive β-cells with quantitative results on the left and representative images on the right. (E) Analysis of high fat fed control and APT1 islet KO mice for percentage of TUNEL positive β-cells with quantitative results on the left and representative images on the right. Scale=50μm.

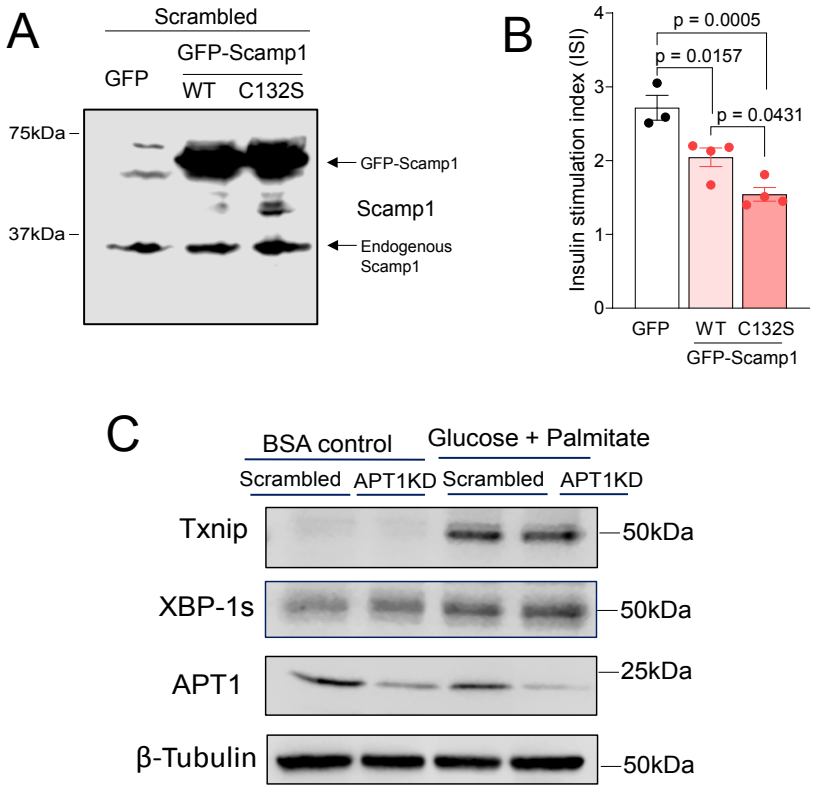

Figure S6. Related to Figure 6. Overexpression of Scamp1 suppresses glucose stimulated insulin secretion in INS-1 cells and characterization of ER stress markers in INS-1 cells. (A) Western blot demonstrating overexpression of wild type and C132S Scamp1 in INS-1 cells without knocking down APT1. (B) Glucose stimulated insulin secretion in INS-1 cells transfected with GFP only, wild type Scamp1, and C132S Scamp1 in cells without knocking down APT1. The greatest degree of suppression of glucose stimulated insulin secretion occurs with the C132S Scamp1 mutant that cannot be palmitoylated. P values represent comparisons by ANOVA. (C) Effects of glucose and palmitate incubation on thioredoxin-interacting protein (Txnip) and the active form of X-box binding protein 1 (XBP-1s) in control/Scrambled and APT1KD INS-1 cells.

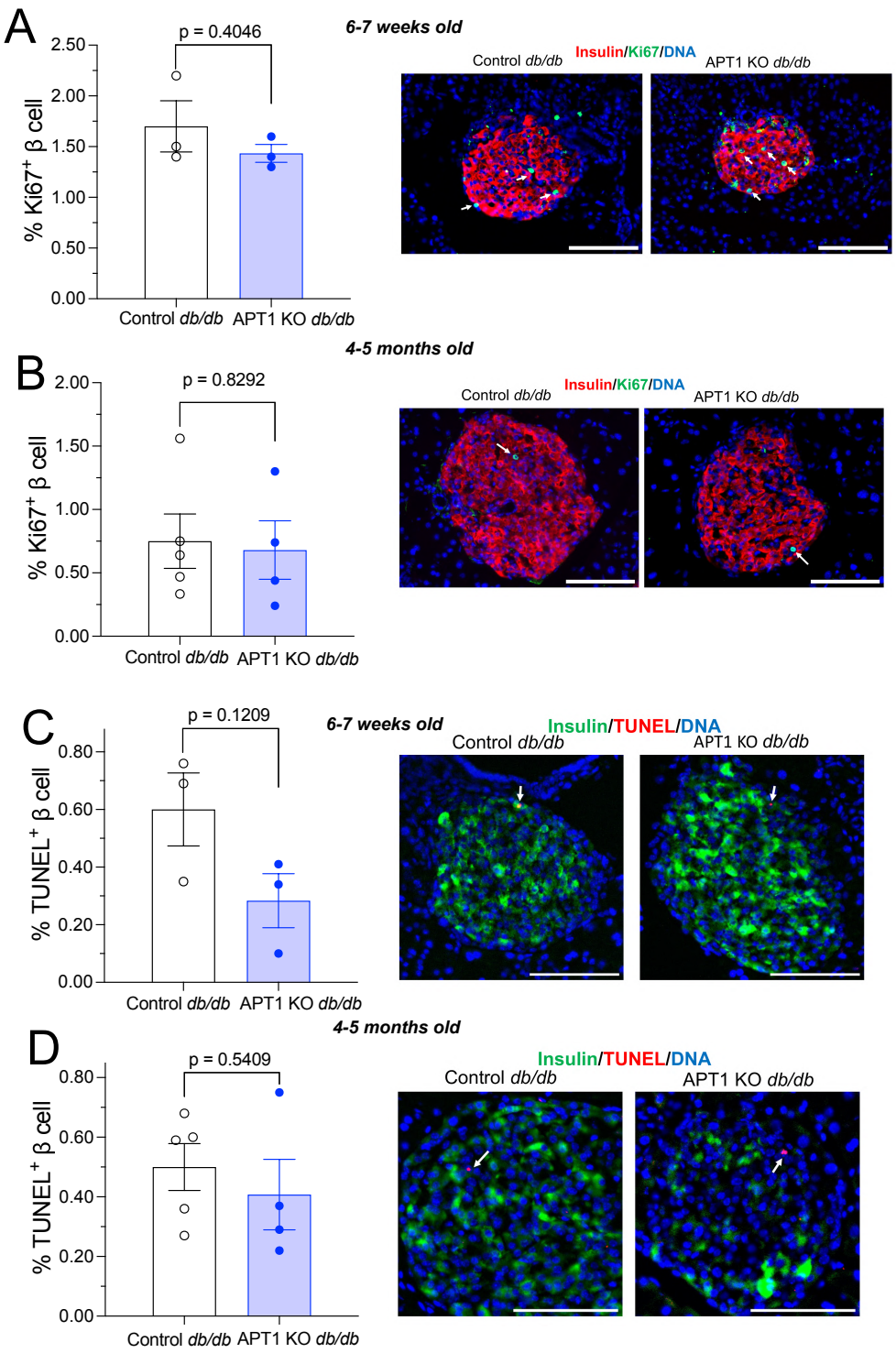

Figure S7. Related to Figure 7. Proliferation and apoptosis in *db/db* islets. (A-B) Analysis of control *db/db* and APT1 KO *db/db* mice for percentage of Ki67 positive β-cells with quantitative results on the left and representative images on the right at the age of 6-7 weeks (A) and the age of 4-5 months (B). (C-D) Analysis of control *db/db* and APT1 KO *db/db* mice for percentage of TUNEL positive β-cells with quantitative results on the left and representative images on the right at the age of 6-7 weeks (C) and the age of 4-5 months (D). Scale=100μm.

Table S1. Human Islet Donor Demographics, Related to Figure 1

A. Donor demographics for APT1 mRNA in human islets.

Group	Nondiabetic	Type 2 Diabetes (T2D)
Sample size	7	4
Gender	4 male, 3 female	3 male, 1 female
Age (years)	44 ± 3, Range 30-56	52 ± 5, Range 40-63
Body weight (kg)	84 ± 7	78 ± 5
BMI	29 ± 2	28 ± 3
HbA1c (%)	5.1 ± 0.1	7.0 ± 0.2
Diabetes medications	None	None-no diabetes by history (3) oral agents (1)
Cause of death	Anoxia (4), CVA (2), Head trauma (1)	Anoxia (3), CVA (1)
Donor ID	HP-18032-01; HP-18063-01; HP-18066-01; HP-18081-01; HP-18110-01; HP-18125-01; HP-18236-01	HP-18038-01T2D; HP-18165-01T2D; HP-18179-01T2D; HP-18212-01T2D

Data expressed as mean ± sem. CVA is cerebrovascular accident (stroke).

B. Donor demographics for APT1 enzyme activity in nondiabetic human islets incubated in high glucose.

	Human islets 1	Human islets 2	Human islets 3
Gender	Female	Female	Male
Age	54	39	21
Body weight (kg)	73	56	79
BMI	25	22	27
HbA1c (%)	5.7	5.6	5.1
Diabetes medications	None	None	None
Cause of death	CVA	Head trauma	Head trauma
Donor ID	HP-20179-01	HP-20191-01	HP-20199-01

CVA is cerebrovascular accident (stroke).

C. Donor demographics for APT1 knockdown in nondiabetic human islets.

	Human islets 1	Human islets 2
Gender	Male	Male
Age	64	37
Body weight (kg)	70	90
BMI	26	24
HbA1c (%)	5.4	5.8
Diabetes medications	None	None
Cause of death	CVA	Head trauma
Donor	HP-19256-01	HP-19276-01

CVA is cerebrovascular accident (stroke)

Table S2. Mouse Phenotyping and Islet Palmitoylation Candidates, Related to Figures 2 and 4

A. Characteristics of global and islet-specific APT1 knockout mice on chow diet.

Parameter	Global KO controls	Global APT1 KO mice	Islet KO controls	Islet-specific APT1 KO mice
Age	5 months	5 months	3 months	3 months
Male weight (g)	27.9 ± 0.7	26.8 ± 0.5	24.1 ± 0.5	23.7 ± 0.5
Female weight (g)	21.2 ± 0.4	19.8 ± 0.4	18.9 ± 0.5	19.4 ± 0.9
Insulin (pg/mL)	2615 ± 217	2972 ± 306	2770 ± 275	2974 ± 135
Glucose(mg/dl)	168 ± 13	152 ± 24	180 ± 11	157 ± 11
Triglycerides (mg/dl)	43 ± 4	44 ± 5	45 ± 2	48 ± 3
Cholesterol (mg/dl)	100 ± 19	96 ± 25	82 ± 12	83 ± 13
NEFA (mM)	0.522 ± 0.011	0.549 ± 0.016	0.456 ± 0.025	0.492 ± 0.021

Data are expressed as mean ± sem (n=4-12 mice per variable). Plasma values were obtained in fasting mice. NEFA is non-esterified fatty acids.

B. Palmitoylation candidates in mouse islets.

Protein Acc	Description	Peptides	Gene	p	Adj p	Log2 Ratio	FC
NP_001002239	Rpl17 ribosomal protein L17 [Mus musculus]	2	*Rpl17*	2.50E-04	1.70E-02	1.66	3.17
NP_036105	Rpl27a ribosomal protein L27a [Mus musculus]	2	*Rpl27a*	4.20E-03	4.40E-02	0.58	1.5
NP_083429	Scamp1 secretory carrier membrane protein 1 [Mus musculus]	3	*Scamp1*	1.30E-03	2.90E-02	1.02	2.03

P values, adjusted p values, log2 ratio and FC (fold change) compare APT1KO and Control.

Table S3. Related to Figure 4

Please see separate Excel file.

Table S4. Related to Figure 4. PCR primers for Scamp1 mutagenesis.

Name	DNA mutation	Location	Sequence (5'-3')
C132S-forward	TGT → TCT	Cytoplasmic	TGGGACCTT**C**TTTCTATCAAGACTTTTCTGTTGACATTCC
C132S-reverse	ACA → AGA		TGATAGAAA**G**AAGGTCCCACGGGAAAATTGCTAGGAAGAG
C170S-forward	TGC → TCC	Transmembrane	TCTTCGGAT**C**CTTGGCCTGGTTTTGTGTTGATTCCTCGAG
C170S-reverse	ACG → AGG		AAACCAGGCCAAG**G**ATCCGAAGATGTTCAGAAACAGGGTC
C175S-forward	TGT → TCT	Transmembrane	GGCCTGGTTTT**C**TGTTGATTCCTCGAGAGCAGTCGACTTT
C175S-reverse	ACA → AGA		GGAATCAACA**G**AAAACCAGGCCAAGCATCCGAAGATGTTC
C197S-forward	TGC → TCC	Transmembrane	TCACTCCCT**C**CTCCTTTGTCTGTTGGTACAGACCGCTGTA
C197S-reverse	ACG → AGG		ACAAAGGAG**G**AGGGAGTGAAGAGCAGGAACCACAGGATGC
C201S-forward	TGT → TCT	Transmembrane	TTTGTCT**C**TTGGTACAGACCGCTGTACGGGGCCTTCAGGA
C201S-reverse	ACA → AGA		GTACCAA**G**AGACAAAGGAGCAGGGAGTGAAGAGCAGGAAC
C227S-forward	TGT → TCT	Transmembrane	TCTATATTT**C**TCAGTTTGCTGTCCATGTGCTCCAGGCTGC
C227S-reverse	ACA → AGA		GCAAACTGA**G**AAATATAGACGAAGAAGAACACAAAGAACC
C245S-forward	TGT → TCT	Lumenal	TGGGGAAACT**C**TGGTTGGATCTCGTCCCTCACTGGTCTCA
C245S-reverse	ACA → AGA		ATCCAACCA**G**AGTTTCCCCAGTTATGAAATCCTGCAGCCT